



# A general class of non-linear kinematic models to predict mean stress relaxation and multiaxial ratcheting in fatigue problems – Part I: Ilyushin spaces <sup>☆</sup>



Marco Antonio Meggiolaro <sup>a,\*</sup>, Jaime Tupiassú Pinho de Castro <sup>a</sup>, Hao Wu <sup>b</sup>

<sup>a</sup> Department of Mechanical Engineering, Pontifical Catholic University of Rio de Janeiro, Rua Marquês de São Vicente, 225 – Gávea, Rio de Janeiro, RJ 22451-900, Brazil

<sup>b</sup> School of Aerospace Engineering and Applied Mechanics, Tongji University 1239 Siping Road, Shanghai, PR China

## ARTICLE INFO

### Article history:

Received 17 November 2014

Accepted 25 August 2015

Available online 9 September 2015

### Keywords:

Multiaxial fatigue

Ratcheting

Incremental plasticity

Non-linear kinematic hardening

Non-proportional loading

## ABSTRACT

Ratcheting is an accumulation of plastic strain that can influence fatigue lives of structural components due to the premature exhaustion of the material ductility, much earlier than predicted by traditional fatigue crack initiation models. Ratcheting is usually associated with a significant mean stress component in either uniaxial or multiaxial stress-controlled histories. The very same process can induce mean stress relaxation in strain-controlled histories, affecting fatigue lives due to consequent mean or maximum stress effects. Such processes are mainly caused by a local distortion of the yield surface, which would require the use of complex yield functions other than von Mises' to be properly described. The addition of non-linear terms to the kinematic hardening rules compensates for this requirement, rendering it possible to model ratcheting effects using the von Mises yield function without dealing with distortion. In this two-part work, the formulation of the main non-linear kinematic (NLK) models is unified into a generalized equation, represented using engineering notation in a reduced-order five-dimensional (5D) space that may lower in half the associated computational cost. Part I introduces the proposed 5D stress and strain spaces, which are a scaled version of Ilyushin's 5D spaces. These 5D spaces are then applied to the qualitative study of uniaxial ratcheting, multiaxial ratcheting, and mean stress relaxation. Part II of this work derives all incremental plasticity equations from the NLK approach in the spaces proposed in Part I, and discusses its advantages over the classical 6D formulation. These NLK models are then used in Part II to quantitatively predict uniaxial ratcheting, multiaxial ratcheting, and mean stress relaxation, validated from experiments with 316L steel cylindrical and tubular specimens.

© 2015 Elsevier Ltd. All rights reserved.

## 1. Introduction

Ratcheting, sometimes called cyclic creep, is the accumulation of any plastic strain component with increasing number of cycles [1]. Although this phenomenon is activated by cyclic plastic loading, it leads to a steady straining in a certain direction that can influence the fatigue life of structural components due to the premature exhaustion of the material ductility, much earlier than its usual fatigue initiation life. It can happen independently of temperature, even though temperature effects can influence ratcheting by

changing the yield strength and the hardening or softening behavior of the material.

Ratcheting is usually associated with uniaxial or multiaxial load histories containing mean stresses. Any loading history that triggers the unsteady effects associated with ratcheting is called an *unbalanced* history. Balanced histories, on the other hand, can also present complex transient elastoplastic hysteresis loops due to strain hardening or softening effects, however after them the material behavior involves a closed elastoplastic loop, with no net accumulation of plastic deformation.

In unbalanced histories, plastic strain accumulation can continue even after the strain hardening or softening transient, generating hysteresis loops that do not fully close. But ratcheting rates might decay as a function of the accumulated plastic strain, until reaching stabilized closed hysteresis loops, in a *plastic shakedown* process. In some cases, it is possible that the steady-state is not

<sup>☆</sup> This paper was submitted for the special issue The Conference of Fatigue Damage of Structural Materials X (FDSM 2014).

\* Corresponding author. Tel.: +55 21 3527 1424; fax: +55 21 3527 1165.

E-mail addresses: [meggi@puc-rio.br](mailto:meggi@puc-rio.br) (M.A. Meggiolaro), [jtcastro@puc-rio.br](mailto:jtcastro@puc-rio.br) (J.T.P. de Castro), [wuhao@tongji.edu.cn](mailto:wuhao@tongji.edu.cn) (H. Wu).

only a closed loop but it is also perfectly elastic, in which case the transient behavior is called *elastic shakedown*.

There are two main types of ratcheting: uniaxial and multiaxial. The first is caused by an unbalanced uniaxial (or any other proportional) history, while the latter requires unbalanced multiaxial non-proportional (NP) conditions, both under stress control. If, on the other hand, the load history is under strain control, then the same microstructural mechanisms that cause uniaxial or multiaxial ratcheting are responsible for gradually reducing mean stress components toward zero. This phenomenon, called *mean stress relaxation*, can be interpreted as an inverse ratcheting problem, which might be present in both uniaxial and multiaxial strain-controlled histories.

In Part I of this two-part work, reduced-order five-dimensional (5D) stress and strain spaces are proposed, which significantly decrease the computational cost in the incremental plasticity formulations required to predict the material behavior subjected to unbalanced histories. Its application to the qualitative description of ratcheting and mean stress relaxation is discussed, while quantitative evaluations are the subject of Part II, which derives the NLK incremental plasticity equations in the proposed 5D spaces. The proposed 5D representation of stresses and strains is presented next.

## 2. Five-dimensional stress and strain formulation

### 2.1. Voigt–Mandel’s notation

Stress and strain tensors can be represented as nine-dimensional (9D) vectors [2], avoiding the need to work with tensor operations. Even better representations were proposed by Voigt and Mandel [3], taking advantage of shear symmetries to express the stress or strains as six-dimensional (6D) vectors. Denoting  $\sigma_i$  and  $s_i$  as the stress components and their deviatoric parts, and analogously  $\varepsilon_i$  and  $e_i$  for strains, then Voigt–Mandel’s vector representation of the stresses, strains, deviatoric stresses, and deviatoric strains, used in this work, become

$$\begin{cases} \vec{\sigma} = [\sigma_x & \sigma_y & \sigma_z & \tau_{xy}\sqrt{2} & \tau_{xz}\sqrt{2} & \tau_{yz}\sqrt{2}]^T \\ \vec{\varepsilon} = [\varepsilon_x & \varepsilon_y & \varepsilon_z & \gamma_{xy}/\sqrt{2} & \gamma_{xz}/\sqrt{2} & \gamma_{yz}/\sqrt{2}]^T \\ \vec{s} = [s_x & s_y & s_z & \tau_{xy}\sqrt{2} & \tau_{xz}\sqrt{2} & \tau_{yz}\sqrt{2}]^T \\ \vec{e} = [e_x & e_y & e_z & \gamma_{xy}/\sqrt{2} & \gamma_{xz}/\sqrt{2} & \gamma_{yz}/\sqrt{2}]^T \end{cases} \quad (1)$$

where  $\tau_{ij}$  and  $\gamma_{ij}$  are shear strain components, and  $T$  stands for the transpose of a vector. Voigt–Mandel’s 6D notation is extensively used in solid mechanics to model stress–strain relations, particularly to improve computational efficiency in numerical structural mechanics software, since it only needs six scalar variables to represent each  $3 \times 3$  tensor.

The  $\sqrt{2}$  terms in Voigt–Mandel’s vector notation makes it geometrically equivalent to the tensor notation. The transformation from 6D stresses or strains to their deviatoric part can be represented by a  $6 \times 6$  projection matrix  $[A_{6D}]$  through  $\vec{s} = A_{6D} \cdot \vec{\sigma}$  and  $\vec{e} = A_{6D} \cdot \vec{\varepsilon}$ , where

$$[A_{6D}] = \begin{bmatrix} 2/3 & -1/3 & -1/3 & 0 & 0 & 0 \\ -1/3 & 2/3 & -1/3 & 0 & 0 & 0 \\ -1/3 & -1/3 & 2/3 & 0 & 0 & 0 \\ 0 & 0 & 0 & 1 & 0 & 0 \\ 0 & 0 & 0 & 0 & 1 & 0 \\ 0 & 0 & 0 & 0 & 0 & 1 \end{bmatrix} \quad (2)$$

If  $\vec{\varepsilon}$  is elastoplastic, then it is possible to represent its elastic and plastic components in Voigt–Mandel’s notation through  $\vec{\varepsilon} = \vec{\varepsilon}_{el} + \vec{\varepsilon}_{pl}$ , where

$$\begin{aligned} \vec{\varepsilon}_{el} &= \left[ \varepsilon_{x_{el}} & \varepsilon_{y_{el}} & \varepsilon_{z_{el}} & \gamma_{xy_{el}}/\sqrt{2} & \gamma_{xz_{el}}/\sqrt{2} & \gamma_{yz_{el}}/\sqrt{2} \right]^T \\ \vec{\varepsilon}_{pl} &= \left[ \varepsilon_{x_{pl}} & \varepsilon_{y_{pl}} & \varepsilon_{z_{pl}} & \gamma_{xy_{pl}}/\sqrt{2} & \gamma_{xz_{pl}}/\sqrt{2} & \gamma_{yz_{pl}}/\sqrt{2} \right]^T \end{aligned} \quad (3)$$

### 2.2. Ilyushin deviatoric spaces

When dealing with multiaxial stress–strain calculations, it is a good idea to work in stress or strain spaces with reduced dimensions, to save computational cost without modifying the results. By working in the deviatoric space, several equations can be simplified, e.g. Hooke’s law becomes a scalar operation instead of involving stiffness matrices. Voigt–Mandel’s 6D *vectorial* representation of the deviatoric stresses  $\vec{s}$  and strains  $\vec{e}$  is a good choice, since it is geometrically equivalent to the deviatoric *tensors*, and Hooke’s law only requires a scalar elastic parameter  $2G$ , where  $G$  is the shear elastic modulus.

As the deviatoric stresses  $s_x$ ,  $s_y$  and  $s_z$  are linearly-dependent, since  $s_x + s_y + s_z = 0$ , it is possible to reduce the deviatoric stress space dimension from 6D to 5D, defining a 5D deviatoric stress vector  $\vec{s}^* = [s_1 \ s_2 \ s_3 \ s_4 \ s_5]^T$  [4]. There are infinite ways to do this, e.g. defining  $s_3$ ,  $s_4$  and  $s_5$  as proportional to the shear stresses  $\tau_{xy}$ ,  $\tau_{xz}$  and  $\tau_{yz}$ , while representing the normal stresses  $\sigma_x$ ,  $\sigma_y$  and  $\sigma_z$  by their hydrostatic component  $\sigma_h$  and two new variables  $s_1$  and  $s_2$ , through

$$\begin{bmatrix} s_1 \\ s_2 \\ \sigma_h \end{bmatrix} = \begin{bmatrix} a_{x1} & a_{y1} & a_{z1} \\ a_{x2} & a_{y2} & a_{z2} \\ 1/3 & 1/3 & 1/3 \end{bmatrix} \cdot \begin{bmatrix} \sigma_x \\ \sigma_y \\ \sigma_z \end{bmatrix} \quad (4)$$

where the user-defined coefficients  $a_{x1}$ ,  $a_{y1}$ ,  $a_{z1}$ ,  $a_{x2}$ ,  $a_{y2}$  and  $a_{z2}$  are values that make the transformation matrix rows  $[a_{x1} \ a_{y1} \ a_{z1}]$ ,  $[a_{x2} \ a_{y2} \ a_{z2}]$ , and  $[1/3 \ 1/3 \ 1/3]$  become linearly independent.

To avoid undesirable geometric distortions in this transformation, the axes associated with  $s_1$ ,  $s_2$  and  $\sigma_h$  should also be orthogonal. Hence, the axes associated with the components  $s_1$  and  $s_2$  should be defined on the deviatoric plane and perpendicular to each other. Using this requirement, a family of coordinate transformations involving a scaling factor  $k_s$  and a rotation angle  $\varphi_s$  can be proposed, see Fig. 1(left), where

$$\begin{aligned} \begin{bmatrix} s_1 \\ s_2 \end{bmatrix} &= \begin{bmatrix} a_{x1} & a_{y1} & a_{z1} \\ a_{x2} & a_{y2} & a_{z2} \end{bmatrix} \cdot \begin{bmatrix} \sigma_x \\ \sigma_y \\ \sigma_z \end{bmatrix} \\ &= k_s \cdot \begin{bmatrix} \cos(\varphi_s) & \cos(\varphi_s + 120^\circ) & \cos(\varphi_s + 240^\circ) \\ \sin(\varphi_s) & \sin(\varphi_s + 120^\circ) & \sin(\varphi_s + 240^\circ) \end{bmatrix} \cdot \begin{bmatrix} \sigma_x \\ \sigma_y \\ \sigma_z \end{bmatrix} \end{aligned} \quad (5)$$

This is a generalization of the classical Ilyushin’s transformations [5], which adopted the particular scaling factor  $k_s = \cos 35.3^\circ = \sqrt{2/3}$ .

Defining  $s_3 \equiv k_s\sqrt{3} \cdot \tau_{xy}$ ,  $s_4 \equiv k_s\sqrt{3} \cdot \tau_{xz}$  and  $s_5 \equiv k_s\sqrt{3} \cdot \tau_{yz}$ , it can be shown that, for any  $\varphi_s$ ,

$$\left. \begin{aligned} s_1^2 + s_2^2 &= k_s^2 \cdot \left( \sigma_x^2 + \sigma_y^2 + \sigma_z^2 - \sigma_x\sigma_y - \sigma_x\sigma_z - \sigma_y\sigma_z \right) \\ s_3^2 + s_4^2 + s_5^2 &\equiv k_s^2 \cdot 3 \left( \tau_{xy}^2 + \tau_{xz}^2 + \tau_{yz}^2 \right) \end{aligned} \right\} \Rightarrow |\vec{s}^*| = \sigma_{Mises} \cdot k_s \quad (6)$$

where  $\sigma_{Mises}$  is the von Mises equivalent stress, and  $|\cdot|$  stands for the Euclidean norm of a vector. Note that Ilyushin’s

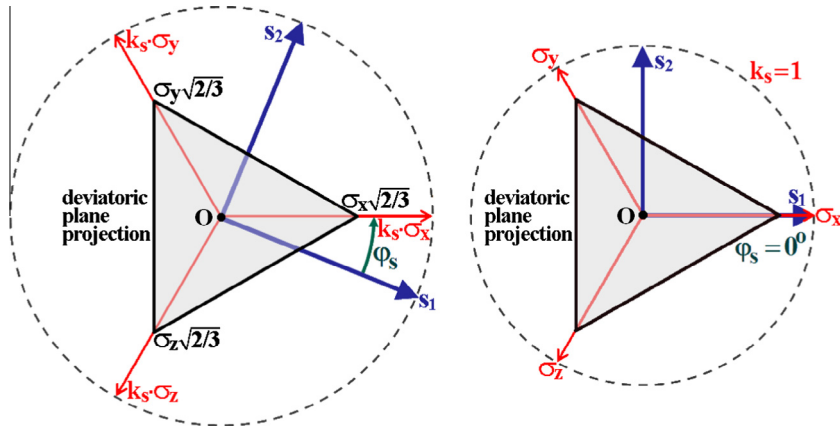


Fig. 1. Coordinate transformations between the normal stresses  $\sigma_x$ ,  $\sigma_y$  and  $\sigma_z$  and the deviatoric stresses  $s_1$  and  $s_2$  on the deviatoric plane, for a generic scaling factor  $k_s$  and rotation angle  $\varphi_s$  (left) and for the adopted  $k_s = 1$  and  $\varphi_s = 0^\circ$  (right).

$k_s = \cos 35.3^\circ = \sqrt{2/3}$  makes the 6D  $\vec{s}$  and the 5D  $\vec{s}^d$  have the same norm.

On the other hand, adopting instead  $k_s = 1$  conveniently results in  $|\vec{s}^d| = \sigma_{Mises}$ . The resulting transformation between the 5D deviatoric stress  $\vec{s}^d$  and the 6D stress  $\vec{\sigma}$  becomes  $\vec{s}^d = A(k_s, \varphi_s) \cdot \vec{\sigma}$ , where the projection matrix  $A(k_s, \varphi_s)$  is given by:

$$\begin{bmatrix} s_1 \\ s_2 \\ s_3 \\ s_4 \\ s_5 \end{bmatrix}_{\vec{s}^d} = k_s \cdot \underbrace{\begin{bmatrix} \cos(\varphi_s) & \cos(\varphi_s + 120^\circ) & \cos(\varphi_s + 240^\circ) & 0 & 0 & 0 \\ \sin(\varphi_s) & \sin(\varphi_s + 120^\circ) & \sin(\varphi_s + 240^\circ) & 0 & 0 & 0 \\ 0 & 0 & 0 & \sqrt{3/2} & 0 & 0 \\ 0 & 0 & 0 & 0 & \sqrt{3/2} & 0 \\ 0 & 0 & 0 & 0 & 0 & \sqrt{3/2} \end{bmatrix}}_{A(k_s, \varphi_s)} \cdot \underbrace{\begin{bmatrix} \sigma_x \\ \sigma_y \\ \sigma_z \\ \tau_{xy}\sqrt{2} \\ \tau_{xz}\sqrt{2} \\ \tau_{yz}\sqrt{2} \end{bmatrix}}_{\vec{\sigma}} \quad (7)$$

Note that the 6D-to-5D projection matrix adopted by Papadopoulos [6] is a particular case of Eq. (7), namely for  $A(k_s = 1/\sqrt{3}, \varphi_s = 0^\circ)$ . The 5D Euclidean sub-space  $E_{5s}$  adopted in this work uses instead a projection matrix  $A(k_s = 1, \varphi_s = 0^\circ)$ , see Fig. 1(right), to make its metric  $|\vec{s}^d|$  equal to  $\sigma_{Mises}$ :

$$\vec{s}^d \equiv \begin{bmatrix} s_1 \\ s_2 \\ s_3 \\ s_4 \\ s_5 \end{bmatrix} = \underbrace{\begin{bmatrix} 1 & -1/2 & -1/2 & 0 & 0 & 0 \\ 0 & \sqrt{3}/2 & -\sqrt{3}/2 & 0 & 0 & 0 \\ 0 & 0 & 0 & \sqrt{3}/2 & 0 & 0 \\ 0 & 0 & 0 & 0 & \sqrt{3}/2 & 0 \\ 0 & 0 & 0 & 0 & 0 & \sqrt{3}/2 \end{bmatrix}}_A \cdot \begin{bmatrix} \sigma_x \\ \sigma_y \\ \sigma_z \\ \tau_{xy}\sqrt{2} \\ \tau_{xz}\sqrt{2} \\ \tau_{yz}\sqrt{2} \end{bmatrix} \equiv A \cdot \vec{\sigma} \quad (8)$$

Such adopted transformation remains unchanged if  $\sigma_x$ ,  $\sigma_y$  and  $\sigma_z$  are replaced respectively by their deviatoric components  $s_x$ ,  $s_y$  and  $s_z$ , therefore

$$\vec{s}^d \equiv [s_1 \ s_2 \ s_3 \ s_4 \ s_5]^T = A \cdot \vec{\sigma} = A \cdot \vec{s} \quad (9)$$

where

$$\begin{aligned} s_1 &\equiv \sigma_x - \frac{\sigma_y + \sigma_z}{2} = \frac{3}{2}s_x, & s_2 &\equiv \frac{\sigma_y - \sigma_z}{2}\sqrt{3} = \frac{s_y - s_z}{2}\sqrt{3} \\ s_3 &\equiv \tau_{xy}\sqrt{3}, & s_4 &\equiv \tau_{xz}\sqrt{3}, & s_5 &\equiv \tau_{yz}\sqrt{3} \end{aligned} \quad (10)$$

The above defined 5D deviatoric stress vector  $\vec{s}^d$  has three important properties:

1. The Euclidean norm of the 5D vector  $\vec{s}^d$  from the  $E_{5s}$  deviatoric sub-space is equal to the von Mises equivalent stress  $\sigma_{Mises}$ , thus

$$|\vec{s}^d| = |\vec{s}|/\sqrt{2/3} = \sigma_{Mises} \equiv \tau_{Mises}\sqrt{3} \quad (11)$$

2. The Euclidean distance in the  $E_{5s}$  space between two stress states (points) A and B, defined by  $\vec{s}_A^d = [s_{1A} \ s_{2A} \ s_{3A} \ s_{4A} \ s_{5A}]^T$  and  $\vec{s}_B^d = [s_{1B} \ s_{2B} \ s_{3B} \ s_{4B} \ s_{5B}]^T$ , respectively associated with the 6D deviatoric stresses  $\vec{s}_A$  and  $\vec{s}_B$ , is equal to the von Mises range  $\Delta\sigma_{Mises}$  between these stress states:

$$|\vec{s}_B^d - \vec{s}_A^d| = |\vec{s}_B - \vec{s}_A|/\sqrt{2/3} = \Delta\sigma_{Mises} \equiv \Delta\tau_{Mises}\sqrt{3} \quad (12)$$

3. The locus of the points that have the same range  $\Delta\sigma_{Mises}$  with respect to a stress state  $\vec{s}^d$  in  $E_{5s}$  is the surface of a hypersphere with center in  $\vec{s}^d$  and radius  $\Delta\sigma_{Mises}$ , a corollary from the second property.

Note that such properties are valid for any projection matrix with a scaling factor  $k_s = 1$ , independently of the choice of  $\varphi_s$ , i.e., for any projection matrix  $A(1, \varphi_s)$ .

### 2.3. Elastic and plastic deviatoric strain spaces

For strain histories, it is also possible to represent the deviatoric strains in 5D strain-based sub-spaces. In this work, the same  $A(1, 0^\circ)$  projection matrix is used for strains, resulting in the 5D Euclidean sub-space  $E_{5e}$  with coordinates

$$\vec{\epsilon}' \equiv [e_1 \ e_2 \ e_3 \ e_4 \ e_5]^T = A \cdot \vec{\epsilon} = A \cdot \vec{\epsilon} \quad (13)$$

where

$$\begin{cases} e_1 \equiv \epsilon_x - \frac{\epsilon_y + \epsilon_z}{2} = \frac{3}{2} \epsilon_x, & e_2 \equiv \frac{\epsilon_y - \epsilon_z}{2} \sqrt{3} = \frac{\epsilon_y - \epsilon_z}{2} \sqrt{3} \\ e_3 \equiv \frac{\gamma_{xy}}{2} \sqrt{3}, & e_4 \equiv \frac{\gamma_{xz}}{2} \sqrt{3}, & e_5 \equiv \frac{\gamma_{yz}}{2} \sqrt{3} \end{cases} \quad (14)$$

This 5D deviatoric strain  $\vec{\epsilon}'$  in the defined sub-space  $E_{5e}$  also has three important properties, very similar to the  $E_{5s}$  stress sub-space properties:

1. The Euclidean norm of the 5D vector  $\vec{\epsilon}'$  divided by  $1 + \bar{\nu}$  is equal to the von Mises equivalent strain  $\epsilon_{Mises}$ :

$$\frac{|\vec{\epsilon}'|}{1 + \bar{\nu}} = \frac{1}{1 + \bar{\nu}} \cdot \frac{|\vec{\epsilon}|}{\sqrt{2/3}} = \epsilon_{Mises} \equiv \frac{1}{1 + \bar{\nu}} \cdot \frac{\gamma_{Mises}}{2} \sqrt{3} \quad (15)$$

where  $\bar{\nu}$  is the effective Poisson ratio, a weighted average between the elastic  $\nu$  and plastic 0.5 Poisson ratios.

2. The Euclidean distance in the  $E_{5e}$  sub-space between two points, divided by  $1 + \bar{\nu}$ , is equal to the von Mises strain range  $\Delta \epsilon_{Mises}$  between these strain states.
3. The locus of the points with same  $\Delta \epsilon_{Mises}$  with respect to a point  $\vec{\epsilon}'$  in the  $E_{5e}$  sub-space is the surface of a 5D hypersphere with center in  $\vec{\epsilon}'$  and radius  $\Delta \epsilon_{Mises} \cdot (1 + \bar{\nu})$ , a corollary from the second property.

The 5D deviatoric stresses and strains proposed above can represent any multiaxial history, even at points below the surface of the specimen. In the particular case of points on a free surface perpendicular to the  $z$  direction, where  $\tau_{xz} = \tau_{yz} = 0$  and  $\gamma_{xz} = \gamma_{yz} = 0$  but allowing  $\sigma_z \neq 0$  (due e.g. to a surface pressure), the proposed deviatoric stress and strain vectors can be further reduced to 3D sub-spaces

$$\begin{cases} \vec{s}_{3D} \equiv [s_1 \ s_2 \ s_3]^T = \left[ \sigma_x - \frac{\sigma_y + \sigma_z}{2} \quad \frac{\sigma_y - \sigma_z}{2} \sqrt{3} \quad \tau_{xy} \sqrt{3} \right]^T \\ \vec{\epsilon}_{3D} \equiv [e_1 \ e_2 \ e_3]^T = \left[ \epsilon_x - \frac{\epsilon_y + \epsilon_z}{2} \quad \frac{\epsilon_y - \epsilon_z}{2} \sqrt{3} \quad \frac{\gamma_{xy}}{2} \sqrt{3} \right]^T \end{cases} \quad (16)$$

Moreover, for surface histories consisting of combinations of only uniaxial tension  $\sigma_x$  and torsion  $\tau_{xy}$ , 2D sub-spaces could be used to simplify even further the representation of the deviatoric stress and strain vectors

$$\begin{cases} \vec{s}_{2D} \equiv [s_1 \ s_3]^T = [\sigma_x \ \tau_{xy} \sqrt{3}]^T \\ \vec{\epsilon}_{2D} \equiv [e_1 \ e_3]^T = \left[ \epsilon_x \cdot (1 + \bar{\nu}) \quad \frac{\gamma_{xy}}{2} \sqrt{3} \right]^T \end{cases} \quad (17)$$

Such simplifications are a major advantage of the  $E_{5s}$  and  $E_{5e}$  spaces. For instance, since the stress component  $\sigma_x$  shows up in all deviatoric components  $s_x$ ,  $s_y$  and  $s_z$ , a simple tension–torsion history would normally need to be represented in a 4D sub-space  $[s_x \ s_y \ s_z \ \tau_{xy} \sqrt{2}]^T$  if Voigt–Mandel's notation was used, instead of the above reduced 2D formulation. Note that, for uniaxial histories, the trivial scalar sub-spaces  $\vec{s}_{1D} \equiv [s_1]$  and  $\vec{\epsilon}_{1D} \equiv [e_1]$  could be adopted.

Instead of having to deal with the effective Poisson ratio  $\bar{\nu}$ , which is an approximation combining the elastic  $\nu$  and plastic 0.5 Poisson ratios, it is much better to represent the deviatoric strain as a sum of its elastic and plastic components  $\vec{\epsilon}' = \vec{\epsilon}_{el} + \vec{\epsilon}_{pl}$  in 5D:

$$\vec{\epsilon}'_{el} \equiv [e_{1el} \ e_{2el} \ e_{3el} \ e_{4el} \ e_{5el}]^T = A \cdot \vec{\epsilon}_{el} = A \cdot \vec{\epsilon}_{el} \quad (18)$$

$$\vec{\epsilon}'_{pl} \equiv [e_{1pl} \ e_{2pl} \ e_{3pl} \ e_{4pl} \ e_{5pl}]^T = A \cdot \vec{\epsilon}_{pl} = A \cdot \vec{\epsilon}_{pl} \quad (19)$$

where  $el$  and  $pl$  subscripts stand respectively for elastic and plastic components, and

$$\begin{cases} e_{1el} \equiv \epsilon_{x_{el}} - \frac{\epsilon_{y_{el}} + \epsilon_{z_{el}}}{2} = \frac{3}{2} \epsilon_{x_{el}}, & e_{2el} \equiv \frac{\epsilon_{y_{el}} - \epsilon_{z_{el}}}{2} \sqrt{3} = \frac{\epsilon_{y_{el}} - \epsilon_{z_{el}}}{2} \sqrt{3} \\ e_{3el} \equiv \frac{\gamma_{xy_{el}}}{2} \sqrt{3}, & e_{4el} \equiv \frac{\gamma_{xz_{el}}}{2} \sqrt{3}, & e_{5el} \equiv \frac{\gamma_{yz_{el}}}{2} \sqrt{3} \end{cases} \quad (20)$$

$$\begin{cases} e_{1pl} \equiv \epsilon_{x_{pl}} - \frac{\epsilon_{y_{pl}} + \epsilon_{z_{pl}}}{2} = \frac{3}{2} \epsilon_{x_{pl}}, & e_{2pl} \equiv \frac{\epsilon_{y_{pl}} - \epsilon_{z_{pl}}}{2} \sqrt{3} = \frac{\epsilon_{y_{pl}} - \epsilon_{z_{pl}}}{2} \sqrt{3} \\ e_{3pl} \equiv \frac{\gamma_{xy_{pl}}}{2} \sqrt{3}, & e_{4pl} \equiv \frac{\gamma_{xz_{pl}}}{2} \sqrt{3}, & e_{5pl} \equiv \frac{\gamma_{yz_{pl}}}{2} \sqrt{3} \end{cases} \quad (21)$$

The 5D plastic strain space defined by  $\vec{\epsilon}'_{pl}$  is hereby called  $E_{5p}$  space. Note that such  $\vec{\epsilon}'_{pl}$  vector, multiplied by  $3/2$ , is identical to the 5D representation of plastic strains proposed by Tanaka [7]:

$$\vec{\epsilon}'_{pl} = \frac{3}{2} \cdot \underbrace{\left[ \epsilon_{x_{pl}} \quad \frac{\epsilon_{y_{pl}} + 2\epsilon_{z_{pl}}}{\sqrt{3}} \quad \frac{\gamma_{xy_{pl}}}{\sqrt{3}} \quad \frac{\gamma_{xz_{pl}}}{\sqrt{3}} \quad \frac{\gamma_{yz_{pl}}}{\sqrt{3}} \right]^T}_{\text{Tanaka's 5D deviatoric space}} \quad (22)$$

since the identity  $\epsilon_{x_{pl}} + \epsilon_{y_{pl}} + \epsilon_{z_{pl}} = 0$  implies that  $\epsilon_{y_{pl}} - \epsilon_{z_{pl}} = \epsilon_{x_{pl}} + 2\epsilon_{y_{pl}}$ . Therefore, Tanaka's efficient non-proportional hardening model [7] can be directly computed in the proposed  $E_{5p}$  formulation, without requiring any additional plastic strain projection.

Similarly to the  $E_{5s}$  stress sub-space, 3D and 2D versions of the strain spaces can also be defined respectively under free-surface and tension–torsion conditions, resulting in

$$\begin{cases} \vec{\epsilon}_{3D_{el}} \equiv \left[ \epsilon_{x_{el}} - \frac{\epsilon_{y_{el}} + \epsilon_{z_{el}}}{2} \quad \frac{\epsilon_{y_{el}} - \epsilon_{z_{el}}}{2} \sqrt{3} \quad \frac{\gamma_{xy_{el}}}{2} \sqrt{3} \right]^T \\ \vec{\epsilon}_{3D_{pl}} \equiv \frac{3}{2} \cdot \left[ \epsilon_{x_{pl}} \quad \frac{\epsilon_{y_{pl}} - \epsilon_{z_{pl}}}{\sqrt{3}} \quad \frac{\gamma_{xy_{pl}}}{\sqrt{3}} \right]^T \end{cases} \quad (23)$$

$$\begin{cases} \vec{\epsilon}_{2D_{el}} \equiv (1 + \nu) \cdot \left[ \epsilon_{x_{el}} \quad \frac{\gamma_{xy_{el}}}{2 \cdot (1 + \nu)} \sqrt{3} \right]^T \\ \vec{\epsilon}_{2D_{pl}} \equiv \frac{3}{2} \cdot \left[ \epsilon_{x_{pl}} \quad \frac{\gamma_{xy_{pl}}}{\sqrt{3}} \right]^T \end{cases} \quad (24)$$

Note that the plastic 2D sub-space where  $\vec{\epsilon}_{2D_{pl}}$  is represented is equivalent to the classic Mises diagram  $\epsilon_{x_{pl}} \times \gamma_{xy_{pl}}/\sqrt{3}$  multiplied by  $3/2$ . But the common practice of representing the elastoplastic strain history in tension–torsion tests using an  $\epsilon_x \times \gamma_{xy}/\sqrt{3}$  diagram is only appropriate if plastic strains dominate, i.e. if  $\epsilon_x \cong \epsilon_{x_{pl}}$ ,  $\gamma_{xy} \cong \gamma_{xy_{pl}}$  and thus  $\vec{\epsilon}_{2D} \cong \vec{\epsilon}_{2D_{pl}}$ . Otherwise,  $\vec{\epsilon}_{2D_{el}}$  and  $\vec{\epsilon}_{2D_{pl}}$  should be studied in separate elastic and plastic diagrams, or altogether in a single elastoplastic diagram  $\vec{\epsilon}_{2D}$  using the effective Poisson ratio.

#### 2.4. Direct and inverse transforms between the adopted 6D and 5D spaces

The inverse transform from the 5D to the 6D space is now calculated using the projection matrix  $A$  defined in Eq. (8). Two important properties of  $A$  are  $A \cdot A^T = 1.5 \cdot I_{5 \times 5}$  and  $A^T \cdot A = 1.5 \cdot A_{6D}$ , where  $I_{5 \times 5}$  is the  $5 \times 5$  identity matrix and  $A_{6D}$  is the projection matrix onto the 6D deviatoric space in Voigt–Mandel's notation, shown in Eq. (2). These identities would also be valid for any other projection matrix  $A(k_s = 1, \varphi_s)$ , independently of the orientation  $\varphi_s$  of the chosen  $s_1$ – $s_2$  coordinate frame. However,  $A$  is a  $5 \times 6$  matrix, thus it cannot be inverted since it is not square. But its *right pseudo-inverse* could be used instead.

The *right pseudo-inverse* of a matrix  $X$ , defined as  $\text{pinv}(X) \equiv X^T \cdot (X \cdot X^T)^{-1}$ , is a generalization of the inverse that is valid even for non-square matrices. If  $X \cdot X^T$  is invertible, then it is easy to show that  $X \cdot \text{pinv}(X) = (X \cdot X^T) \cdot (X \cdot X^T)^{-1}$  is equal to the identity matrix, analogously to the properties of a square inverse matrix. The *right pseudo-inverse* of  $A$  becomes then

$$\text{pinv}(A) \equiv A^T \cdot (A \cdot A^T)^{-1} = A^T \cdot (1.5 \cdot I_{5 \times 5})^{-1} = 1.5 \cdot A^T \quad (25)$$

which can be used to calculate the inverse transform from the considered 5D stress sub-space back to 6D. But, even though  $\vec{\sigma} = A \cdot \vec{\sigma}$ ,

in general it is not true that  $pinv(A) \cdot \vec{s}$  is equal to the original 6D stress  $\vec{\sigma}$ . Instead, this product results in the 6D deviatoric stress  $\vec{s}$

$$\begin{aligned} pinv(A) \cdot \vec{s} &= \frac{2}{3} A^T \cdot (A \cdot \vec{\sigma}) = \frac{2}{3} \cdot \frac{3}{2} A_{6D} \cdot \vec{\sigma} = \vec{s} \Rightarrow \vec{s} \\ &= pinv(A) \cdot \vec{s} \end{aligned} \quad (26)$$

The reconstruction of the 6D  $\vec{\sigma}$  would also require the knowledge of the 6D hydrostatic stress vector  $\vec{\sigma}_h = \sigma_h \cdot [1 \ 1 \ 1 \ 0 \ 0 \ 0]^T$  to obtain  $\vec{\sigma} = \vec{s} + \vec{\sigma}_h$ . In an analogous way as done for stresses, the pseudo-inverse can also be used to project 5D strains back to their 6D space. The direct and inverse transformations using the proposed projection matrix  $A$  are summarized in Tables 1 and 2.

In summary, the 5D representation of stresses and strains is highly recommended, since it reduces the dimensionality of the stress–strain relations from 6D to 5D. For either free-surface conditions, un-notched tension–torsion, or uniaxial histories, respectively 3D, 2D, or 1D sub-spaces of the 5D representation can be used, significantly decreasing computational cost. Recall that, even for a uniaxial history in  $x$ , Voigt–Mandel's 6D deviatoric representation would need to use three dimensions due to its redundant formulation, since  $\sigma_x$  is present in all three normal deviatoric components  $s_x$ ,  $s_y$  and  $s_z$ . On the other hand, with a uniaxial  $\sigma_x$  present only in the  $s_1$  expression, the 5D representation could use a single component in this case without problems.

The proposed 5D stress and strain formulation will be used in Part II of this paper to better describe non-linear incremental plasticity models, which are required for predicting ratcheting and

mean stress relaxation effects. Such effects are discussed next, in the light of the proposed 5D formulation.

### 3. Uniaxial ratcheting behavior and definitions

Uniaxial unbalanced histories are essentially cyclic histories with a significant mean stress component. Such histories may present plastic strain accumulation in the direction of the mean stress, called uniaxial ratcheting. Uniaxial ratcheting is a result of a different non-linear behavior of the material in tension and in compression, i.e. anisotropy between tension and compression. Masing [8] assumed that the elastoplastic hysteresis loop curves should be geometrically similar to the cyclic stress–strain curves magnified by a scale factor of two, implying that cyclically-stabilized constant-amplitude elastoplastic loops should always close. Uniaxial ratcheting behavior, however, is one in which the steady-state of a cyclic uniaxial loading is an elastoplastic loop that does not close, causing the material to accumulate a net strain during each cycle. From a microscopic point of view, this non-Masing behavior indicates an unstable microstructure in the fatigue process.

Consider the uniaxial load history shown in Fig. 2, with stresses varying between a peak  $\vec{s}_{1D} = [\sigma_{max}]$  ( $\sigma_{max} > S_{Yc}$ ) and a valley  $\vec{s}_{1D} = [-S_{Yc}]$ , where  $S_{Yc}$  is the cyclically-stabilized yield strength. For simplicity, the material stress–strain behavior is assumed bilinear and without any isotropic hardening transient. The stress levels reproduced in Fig. 2 are compatible with kinematic hardening, where yielding in the opposite direction occurs after a stress variation  $\Delta\sigma_x = \pm 2S_{Yc}$ , but the hysteresis loops do not close. This is caused by a non-Masing behavior, where plastic straining along

**Table 1**

Direct and inverse matrix transforms between Voigt–Mandel's 6D and the proposed 5D spaces, where  $A \cdot A^T = 1.5 \cdot I_{5 \times 5}$  and  $A^T \cdot A = 1.5 \cdot A_{6D}$ .

Transform	From 6D to 5D	From 5D to 6D
Stress	$\vec{s} = A \cdot \vec{\sigma} = A \cdot \vec{s} = A' \cdot \vec{s}$	$\vec{s} = (2/3)A^T \cdot \vec{\sigma} \Rightarrow \vec{\sigma} = \vec{s} + \vec{\sigma}_h$
Elastoplastic strain	$\vec{e} = A \cdot \vec{e} = A \cdot \vec{e}$	$\vec{e} = (2/3)A^T \cdot \vec{e} \Rightarrow \vec{e} = \vec{e} + \vec{e}_h$
Elastic strain	$\vec{e}'_{el} = A \cdot \vec{e}_{el} = A \cdot \vec{e}_{el}$	$\vec{e}_{el} = (2/3)A^T \cdot \vec{e}'_{el} \Rightarrow \vec{e}_{el} = \vec{e}_{el} + \vec{e}_h$
Plastic strain	$\vec{e}'_{pl} = A \cdot \vec{e}_{pl} = A \cdot \vec{e}_{pl}$	$\vec{e}_{pl} = \vec{e}'_{pl} = (2/3)A^T \cdot \vec{e}'_{pl}$ (since $\vec{e}_h$ is elastic)

**Table 2**

Direct and inverse scalar transformations between the 6D and 5D representations.

Transform	From 6D to 5D	From 5D to 6D
Stress	$s_1 = \sigma_x - (\sigma_y + \sigma_z)/2$ $s_2 = (\sigma_y - \sigma_z)\sqrt{3}/2$ $s_3 = \tau_{xy}\sqrt{3}$ , $s_4 = \tau_{xz}\sqrt{3}$ $s_5 = \tau_{yz}\sqrt{3}$	$\sigma_x = \sigma_h + s_1 \cdot 2/3$ $\sigma_y = \sigma_h - s_1/3 + s_2/\sqrt{3}$ $\sigma_z = \sigma_h - s_1/3 - s_2/\sqrt{3}$ $\tau_{xy} = s_3/\sqrt{3}$ , $\tau_{xz} = s_4/\sqrt{3}$ , $\tau_{yz} = s_5/\sqrt{3}$
Elastoplastic strain	$e_1 = \epsilon_x - (\epsilon_y + \epsilon_z)/2$ $e_2 = (\epsilon_y - \epsilon_z)\sqrt{3}/2$ $e_3 = \gamma_{xy}\sqrt{3}/2$ $e_4 = \gamma_{xz}\sqrt{3}/2$ $e_5 = \gamma_{yz}\sqrt{3}/2$	$\epsilon_x = \epsilon_h + e_1 \cdot 2/3$ $\epsilon_y = \epsilon_h - e_1/3 + e_2/\sqrt{3}$ $\epsilon_z = \epsilon_h - e_1/3 - e_2/\sqrt{3}$ $\gamma_{xy} = e_3 \cdot 2/\sqrt{3}$ , $\gamma_{xz} = e_4 \cdot 2/\sqrt{3}$ $\gamma_{yz} = e_5 \cdot 2/\sqrt{3}$
Elastic strain	$e'_{1el} = \epsilon_{x'el} - (\epsilon_{y'el} + \epsilon_{z'el})/2$ $e'_{2el} = (\epsilon_{y'el} - \epsilon_{z'el})\sqrt{3}/2$ $e'_{3el} = \gamma_{xy'el}\sqrt{3}/2$ $e'_{4el} = \gamma_{xz'el}\sqrt{3}/2$ $e'_{5el} = \gamma_{yz'el}\sqrt{3}/2$	$\epsilon_{x'el} = \epsilon_h + e'_{1el} \cdot 2/3$ $\epsilon_{y'el} = \epsilon_h - e'_{1el}/3 + e'_{2el}/\sqrt{3}$ $\epsilon_{z'el} = \epsilon_h - e'_{1el}/3 - e'_{2el}/\sqrt{3}$ $\gamma_{xy'el} = e'_{3el} \cdot 2/\sqrt{3}$ , $\gamma_{xz'el} = e'_{4el} \cdot 2/\sqrt{3}$ $\gamma_{yz'el} = e'_{5el} \cdot 2/\sqrt{3}$
Plastic strain	$e'_{1pl} = \epsilon_{x'pl} - (\epsilon_{y'pl} + \epsilon_{z'pl})/2$ $e'_{2pl} = (\epsilon_{y'pl} - \epsilon_{z'pl}) \cdot \sqrt{3}/2$ $e'_{3pl} = \gamma_{xy'pl} \cdot \sqrt{3}/2$ $e'_{4pl} = \gamma_{xz'pl} \cdot \sqrt{3}/2$ $e'_{5pl} = \gamma_{yz'pl} \cdot \sqrt{3}/2$	$\epsilon_{x'pl} = e'_{1pl} \cdot 2/3$ $\epsilon_{y'pl} = -e'_{1pl}/3 + e'_{2pl}/\sqrt{3}$ $\epsilon_{z'pl} = -e'_{1pl}/3 - e'_{2pl}/\sqrt{3}$ $\gamma_{xy'pl} = e'_{3pl} \cdot 2/\sqrt{3}$ , $\gamma_{xz'pl} = e'_{4pl} \cdot 2/\sqrt{3}$ $\gamma_{yz'pl} = e'_{5pl} \cdot 2/\sqrt{3}$

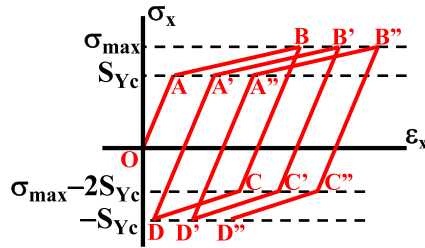


**Fig. 2.** Uniaxial ratcheting for a bi-linear material subjected to an unbalanced stress history between  $\sigma_{max} > S_{Yc}$  and  $-S_{Yc}$ , under stress control, in the absence of strain hardening or softening.

the path AB is larger than in CD, even though both paths are subjected to the same stress variation. This non-Masing asymmetrical behavior causes the slope of the tension path AB to be lower than the slope of the compression path CD, resulting in a net increase in plastic strain after each loop. Note that such increase in plastic strain levels cannot be explained by isotropic softening, since all paths AB, A'B' and A''B'' are parallel, representing a stabilized strain hardening/softening behavior. Similarly, paths CD, C'D' and C''D'' are also parallel, even though they are not parallel to AB due to the non-Masing behavior.

Since isotropic softening under stress control can also cause a net increase in plastic strain per loading cycle, it is useful to separate ratcheting from isotropic softening effects by defining the ratcheting strain as the mean strain along each cycle. In Fig. 2, the ratcheting strain  $\epsilon_{ri}$  is thus defined after the first cycle as  $\epsilon_{r1} = (\epsilon_B + \epsilon_D)/2$ , after the second cycle as  $\epsilon_{r2} = (\epsilon_{B'} + \epsilon_{D'})/2$ , after the third as  $\epsilon_{r3} = (\epsilon_{B''} + \epsilon_{D''})/2$ , and so on. The ratcheting rate per cycle  $d\epsilon/dN$  is then the difference  $d\epsilon/dN = (\epsilon_{ri+1} - \epsilon_{ri})$  between the ratcheting strains from consecutive cycles.

This definition of the ratcheting rate is able to only account for the non-Masing asymmetrical behavior. It is independent of any isotropic transient, since isotropic hardening or softening in fully-reversed (zero mean stress) tension–compression under stress control would result in zero mean strains, therefore  $\epsilon_{ri} = 0$  and thus  $d\epsilon/dN = 0$ , even though there is an increase (or decrease) of the maximum strain per cycle due to cyclic softening (or hardening, respectively).

In summary, cyclic softening and ratcheting are two different processes, the first caused by a symmetrical softening behavior in both tension and compression, and the second by a tension–compression asymmetry in the stress–strain behavior that may happen even after the strain hardening/softening transient. Both effects should be separately modeled to independently predict their similar capability to cause a net increase in plastic strain per loading cycle, even though sometimes their effects are shown superposed in the literature and simply called a ratcheting process.

The ratcheting rate  $d\epsilon/dN$  increases with both the stress range and the mean stress [9], however it is much more sensitive to

the mean stress [10]. The ratcheting rate usually varies with the number of cycles, even for constant amplitude loadings. For high stress ranges, the ratcheting rate  $d\epsilon/dN$  tends to increase at each cycle, until the component fails due to exhaustion of the material ductility, see Fig. 3(a). For lower stress ranges, the ratcheting rate tends to decrease until reaching steady-state with  $d\epsilon/dN = 0$ , associated with a stable hysteresis loop that fully closes, see Fig. 3(b). Note also that uniaxial ratcheting may induce a significant increase in dislocation density when compared to zero-mean-strain low-cycle fatigue loading, which can cause an additional strain-hardening in certain materials, as reported in [11].

**4. Multiaxial ratcheting analysis using deviatoric spaces**

Multiaxial load histories can also result in plastic strain accumulation along a certain direction, a phenomenon called multiaxial ratcheting. Multiaxial ratcheting happens for unbalanced histories even if the material follows the Masing behavior, without any asymmetry in the hysteresis loops under tension and compression. The most common multiaxial ratcheting example can be seen in Fig. 4, which shows an elastoplastic cyclic torsion history with amplitude  $\tau_a$  applied to a shaft, combined with a constant axial stress  $\sigma_m$  (a static “mean” stress). This example can adopt a 2D sub-space of the defined  $E_{5s}$  space, representing stress states in an  $s_1 \times s_3$  diagram from the 2D vector  $\vec{s}_{2D}$  defined in Eq. (17).

Initially, the uniaxial path  $OO'$  causes elastic straining in the normal direction  $[s_1 \ 0]^T$  until  $\sigma_m$  is reached, in a linear elastic process inside the yield surface. The yield surface is the locus of all points associated with a yielding criterion, which in this example is a circle since it is defined from the von Mises criterion  $|\vec{s}_{2D}| = S$ , where  $S$  is the monotonic or cyclic yield strength. Since the path  $O'A_0$  is inside the yield surface, it will cause an elastic shear strain, but without any axial component.

After the stress state reaches the yield surface at point  $A_0$ , the yield surface starts translating toward point A, during which plastic straining occurs. In most materials, such plastic straining happens along a direction  $\vec{n}_A$  normal to the yield surface, what is known as the normality condition or normality rule, discussed in detail in Part II of this work. Since the normal vector  $\vec{n}_A$  is not vertical in the example from Fig. 4(a), plastic straining along the path  $A_0A$  will not only induce an elastoplastic shear level  $\gamma_a$ , but it will also cause a purely plastic tensile strain increment (the ratcheting increment), where the resulting strain path describes a slope in the  $\epsilon_x \times \gamma_{xy}/\sqrt{3}$  diagram approximately equal to the slope of  $\vec{n}_A$ .

The path  $A_0A$  causes the yield surface to translate until its center (the backstress) reaches the position  $\vec{\beta}_{2D} = [0 \ \beta_3]^T$  in the 2D sub-space shown in Fig. 4(b), where  $\beta_3$  is the torsional component of the backstress vector in this  $s_1 \times s_3$  diagram. Elastic unloading of the shear component follows along the path  $AB_1$ , until the stress state reaches the translated surface at  $B_1$ , associated with a normal vector  $\vec{n}_B$ . Then, the yield surface starts translating toward point B,

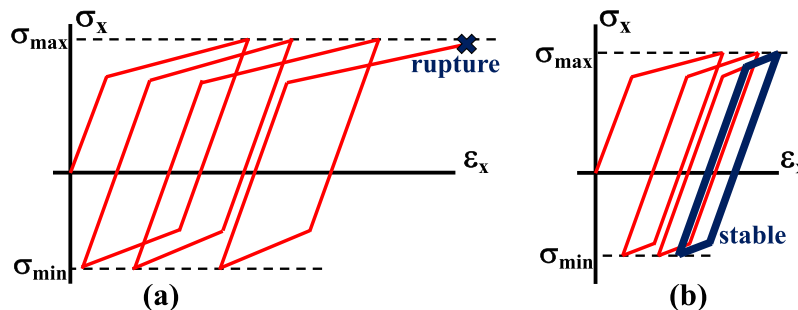


**Fig. 3.** Uniaxial ratcheting for a bi-linear material subjected to an unbalanced stress-controlled history under (a) high stress ranges; (b) low stress ranges.

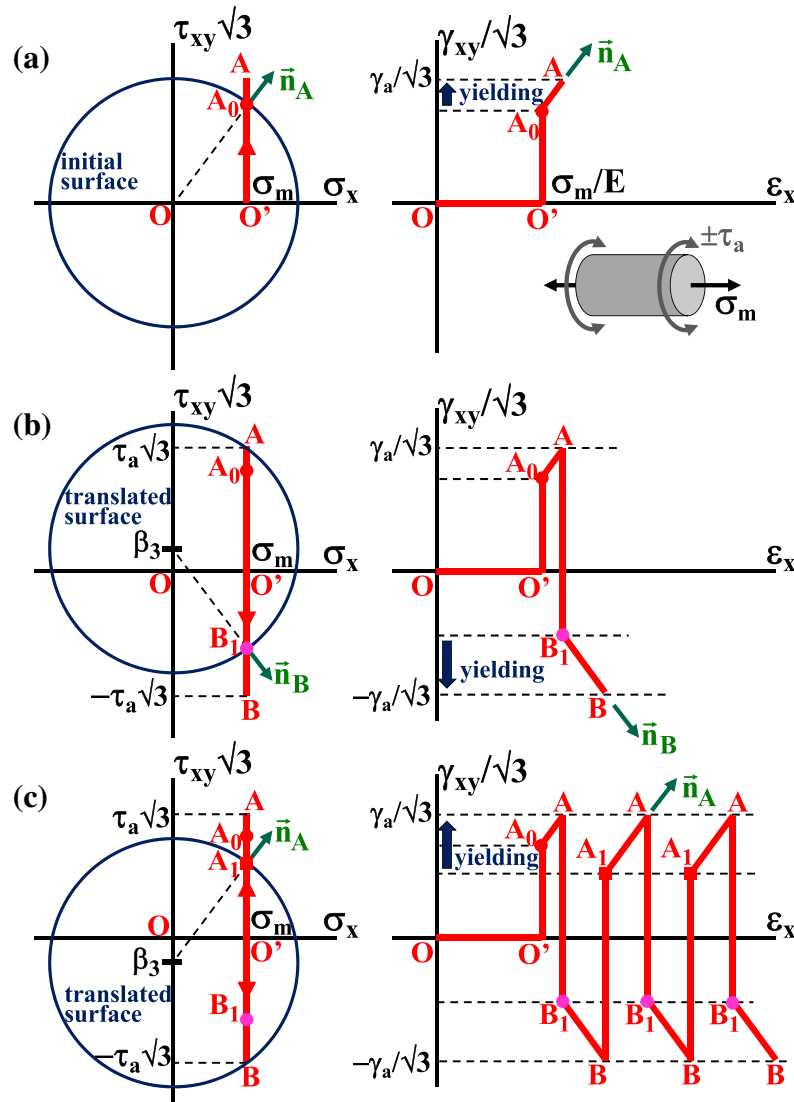


Fig. 4. Cyclic torsion history with shear amplitude  $\tau_a$  and constant axial stress  $\sigma_m$  applied to a shaft, defined by the path  $ABA$  in the  $\bar{s}_{2D}$  diagram  $\sigma_x \times \tau_{xy}/\sqrt{3}$ , and resulting multiaxial ratcheting in the axial direction of the  $\epsilon_x \times \gamma_{xy}/\sqrt{3}$  diagram.

causing plastic straining in both shear and axial components, along a direction in the  $\epsilon_x \times \gamma_{xy}/\sqrt{3}$  diagram approximately equal to the direction of  $\bar{n}_B$ , see Fig. 4(b).

Fig. 4(c) shows the translated yield surface after the stress state reaches  $B$ , with center at a new backstress  $\vec{\beta}_{2D} = [0 \ \beta_3]^T$  with  $\beta_3 < 0$ . Elastic loading follows along the path  $BA_1$ , until reaching again the yield surface at point  $A_1$ . Yielding along the path  $A_1A$  causes once again ratcheting, associated with the slope  $\bar{n}_A$ . The process continues, resulting in this example in a constant ratcheting rate, see Fig. 4(c). Note that yielding occurs at point  $A_0$  only in the first cycle, while in all subsequent cycles it will happen at the  $A_1$  stress state due to the kinematic hardening process.

In this example, yield surface translations were all assumed in the vertical (shear) direction. However, the surface translation direction in most materials is a function of the directions of the normal vectors  $\bar{n}_A$  or  $\bar{n}_B$  and of the backstress vector  $\vec{\beta}$ , as it will be detailed in Part II of this work. The actual surface translation direction ends up changing the directions of  $\bar{n}_A$  and  $\bar{n}_B$  in the subsequent cycles, which in turn will change the translation direction, in a highly-coupled plasticity process. When improved surface translation equations are used to model these effects, it is found

that the ratcheting rate may vary from cycle to cycle instead of being constant.

Ratcheting is also an important problem in pressure vessels or pressurized pipelines that suffer cyclic shear, tension, or bending. Internal pressure causes a hoop stress  $\sigma_\theta$  that acts as the mean component associated with ratcheting problems. If the combination of  $\sigma_\theta$  with the cyclic shear, tension, or bending stresses causes cyclic yielding, then ratcheting may occur in the hoop direction after each loading cycle, causing the vessel pipe to radially expand until eventually exhausting its ductility. Increasing ovalization of the cross section may also happen under cyclic bending, since the vessel/pipe walls will only suffer ratcheting in the highly stressed regions farther away from the neutral bending axis.

In the tension–torsion shaft example, the stress state and yield surface were represented in the usual diagram  $s_1 \times s_3 \equiv \sigma_x \times \tau_{xy}/\sqrt{3}$ , a sub-space of the  $E_{5s}$  stress space, since there were no other normal (or shear) components  $\sigma_y$  or  $\sigma_z$ . However, for cyclic tension or bending problems on a pressurized vessel/pipe, which involve three normal components  $\sigma_x$ ,  $\sigma_\theta$ , and  $\sigma_z$  acting on the inner walls, another sub-space of  $E_{5s}$  needs to be used instead, the stress diagram  $s_1 \times s_2$  defined by the deviatoric components  $s_1 \equiv \sigma_x - (\sigma_\theta + \sigma_z)/2$  and  $s_2 \equiv (\sigma_\theta - \sigma_z)/2$ , where  $\sigma_z = -p$  accounts

for the compressive stresses on such inner walls under a pressure  $p > 0$ . Even though a different sub-space of the  $E_{5s}$  stress space would be adopted, a behavior very similar to the one illustrated in Fig. 4 could be obtained. The use of the 5D formulation or its sub-spaces makes it systematic to predict ratcheting effects, with the ability to consider altogether all 6D stress or strain components, as long as a proper kinematic hardening model is adopted [12, 13], as studied in Part II of this work.

## 5. Mean stress relaxation under strain control

Mean stress relaxation happens during strain-controlled deformation with an initial mean stress [14], being closely related to ratcheting. The mean stress gradually relaxes toward zero, both in uniaxial and multiaxial unbalanced histories. Consider the strain-controlled uniaxial history shown in Fig. 5, applied to the same bi-linear material from Figs. 2–4, without isotropic hardening transients. Non-Masing behavior causes the slope of paths AB, A'B' and A''B'' to be smaller than the slopes of CD, C'D' and C''D'', resulting in an asymmetrical behavior with open hysteresis loops that gradually decrease the mean stress component. As the mean stress tends toward zero, the non-Masing behavior diminishes, making the hysteresis loops become once again symmetric and closed.

Mean stress relaxation caused by high plastic strain ranges is one of the reasons why low-cycle fatigue lives are less influenced by the mean stress effect than high-cycle fatigue lives. It can also explain why the mean stress correction in the plastic term of Morrow's elastoplastic strain-life curve is usually very conservative.

Isotropic hardening and softening compete with mean stress relaxation mechanisms in strain-controlled cyclic deformations of structural alloys. To separate their effects, it is necessary to evaluate the relaxation of the mean stress, not of the maximum stress. Strain-controlled isotropic softening causes a gradual reduction of the maximum stress even in the absence of mean stress relaxation. Hence, the transient effects of mean stress relaxation and isotropic strain softening/hardening can be separated in uniaxial histories by studying, respectively, the evolution of the mean stress and the variation of the stress amplitude or range.

Mean stress relaxation is also found in multiaxial histories, caused by yield surface translations in unbalanced strain-controlled paths. It is present as well in multiaxial elastoplastic paths with mixed stress and strain control, as long as the relaxation direction is under strain control with an initial mean stress. For instance, exposed portions of buried pipelines may bear high static tensile and bending stresses in the axial direction due to ground or seabed displacements. Axial loadings in such long pipelines are

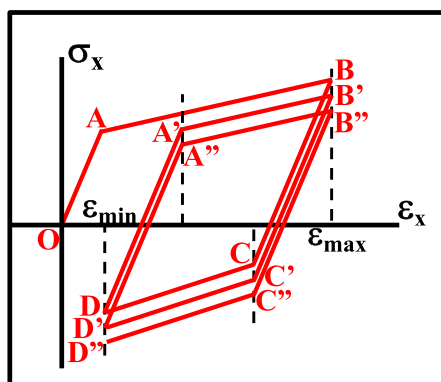


Fig. 5. Uniaxial mean stress relaxation for a bi-linear material subjected to an unbalanced strain history between  $\epsilon_{min}$  and  $\epsilon_{max}$  under strain control.

usually assumed as strain controlled, therefore superimposed pressure cycles that cause plastic straining may result in a gradual relaxation of the axial stresses, increasing the fatigue life. Even though both hoop and radial histories are stress-controlled in the exposed pipeline portion due to the applied internal pressure, mean stress relaxation may happen in the strain-controlled axial direction of such partially-buried pipeline.

Mean stress relaxation can be quantitatively predicted from incremental plasticity simulations [15], if non-linear kinematic models are used to describe the associated asymmetrical behavior of the stress-strain curves, as studied in Part II of this work.

## 6. Conclusions

In this work, five-dimensional (5D) stress and strain spaces were proposed, representing a scaled version of Ilyushin's 5D spaces. These 5D spaces have several important properties, such as a metric proportional to von Mises equivalent stresses or strains, the ability to represent yield surfaces using simple equations without scaling factors, and the possibility to work in reduced-order sub-spaces under free-surface conditions by simply removing appropriate rows from the stress and strain vectorial representations. The transformations to and from the proposed 5D spaces have been presented, providing an efficient framework to define incremental plasticity equations. These 5D spaces were applied to the qualitative study of uniaxial ratcheting, multiaxial ratcheting, and mean stress relaxation, through tension-torsion loading examples in 2D sub-spaces, and an unbalanced stress-controlled uniaxial loading example with significant mean stress. In Part II, a computationally-efficient incremental plasticity formulation is presented in the proposed 5D spaces, with the ability to model isotropic, non-proportional and non-linear kinematic hardening and thus to quantitatively predict ratcheting and mean stress relaxation effects, as verified from experimental measurements.

## Acknowledgments

This work was supported in part by the National Natural Science Foundation of P.R. China under Grant No. 11302150. CNPq-Brazil provided fellowships for Profs. Marco A. Meggiolaro, and Jaime T.P. Castro.

## References

- [1] Kang G. Ratcheting: recent progresses in phenomenon observation, constitutive modeling and application. *Int J Fatigue* 2008;30:1448–72.
- [2] Ilyushin AA. *Plasticité*. Paris: Éditions Eyrolles; 1956.
- [3] Mandel J. *Cours de Mécanique des Milieux Continus, tomes I and II*. Paris: Gauthier-Villars; 1966.
- [4] Bishop JE. Characterizing the non-proportional and out-of-phase extend of tensor paths. *Fatigue Fract Eng Mater Struct* 2000;23:1019–32.
- [5] Ilyushin AA. On the foundations of the general mathematical theory of plasticity. In: *Voprosy Teorii Plastichnosti*, Moskva: Izd. AN SSSR; 1961. p. 3–29 [in Russian].
- [6] Papadopoulos IV, Davoli P, Gorla C, Filippini M, Bernasconi A. A comparative study of multiaxial high-cycle fatigue criteria for metals. *Int J Fatigue* 1997;19:219–35.
- [7] Tanaka E. A nonproportionality parameter and a cyclic viscoplastic constitutive model taking into account amplitude dependences and memory effects of isotropic hardening. *Eur J Mech – A/Solids* 1994;13:155–73.
- [8] Masing G. *Eigenspannungen und Verfestigung Beim Messing*. In: *Proceedings of the 2nd international congress of applied mechanics, Zurich, Switzerland; 1926* [in German].
- [9] Lim C-B, Kim KS, Seong JB. Ratcheting and fatigue behavior of a copper alloy under uniaxial cyclic loading with mean stress. *Int J Fatigue* 2009;31(3):501–7.
- [10] Wang Y, Yu D, Chen G, Chen X. Effects of pre-strain on uniaxial ratcheting and fatigue failure of Z2CN18.10 austenitic stainless steel. *Int J Fatigue* 2013;52:106–13.
- [11] Facheris G, Janssens KGF. Cyclic mechanical behavior of 316L: uniaxial LCF and strain-controlled ratcheting tests. *Nucl Eng Des* 2013;257:100–8.
- [12] Chaboche JL. A review of some plasticity and viscoplasticity constitutive theories. *Int J Plast* 2008;24(10):1642–93.

- [13] Facheris G, Janssens KGF, Foletti S. Multiaxial fatigue behavior of AISI 316L subjected to strain-controlled and ratcheting paths. *Int J Fatigue* 2014;68:195–208.
- [14] Arcari A, De Vita R, Dowling NE. Mean stress relaxation during cyclic straining of high strength aluminum alloys. *Int J Fatigue* 2009;31(11–12):1742–50.
- [15] Landersheim V, Bruder T, Hanselka H. Approximation of mean stress relaxation by numerical simulation using the Jiang model and extrapolation of results. *Procedia Eng* 2011;10:595–600.